

SECOND LAYER NUCLEATION AND THE SHAPE OF WEDDING CAKES

J. Krug and P. Kuhn

Fachbereich Physik, Universität Essen, 45117 Essen, Germany

The rate of second layer nucleation – the formation of a stable nucleus on top of a two-dimensional island – determines both the conditions for layer-by-layer growth, and the size of the top terrace of multilayer mounds in three-dimensional homoepitaxial growth. It was recently shown that conventional mean field nucleation theory overestimates the rate of second layer nucleation by a factor that is proportional to the number of times a given site is visited by an adatom during its residence time on the island. In the presence of strong step edge barriers this factor can be large, leading to a substantial error in previous attempts to experimentally determine barrier energies from the onset of second layer nucleation. In the first part of the paper simple analytic estimates of second layer nucleation rates based on a comparison of the relevant time scales will be reviewed. In the main part the theory of second layer nucleation is applied to the growth of multilayer mounds in the presence of strong but finite step edge barriers. The shape of the mounds is obtained by numerical integration of the deterministic evolution of island boundaries, supplemented by a rule for nucleation in the top layer. For thick films the shape converges to a simple scaling solution. The scaling function is parametrized by the coverage θ_c of the top layer, and takes the form of an inverse error function cut off at θ_c . The surface width of a film of thickness d is $\sqrt{(1 - \theta_c)d}$. Finally, we show that the scaling solution can be derived also from a continuum growth equation.

I. INTRODUCTION

An atom adsorbed on a crystal surface can move from one atomic layer to another (usually from a higher layer to a lower one) only by crossing a step. Irrespective of whether it occurs by simple hopping or by concerted exchange, step crossing is often associated with an additional energy barrier ΔE_S , which reduces the effective rate of interlayer transport, ν' , below the rate ν for adatom diffusion within one atomic layer [1,2]. Here we are assuming conventional Arrhenius laws for ν and ν' ,

$$\nu = \nu_0 e^{-E_D/k_B T}, \quad \nu' = \nu'_0 e^{-E_S/k_B T} \quad (1)$$

and define $\Delta E_S = E_S - E_D$. The consequences for multilayer growth are twofold. On the one hand, the confinement of atoms on top of the two-dimensional islands which form during the growth of the first layer increases the nucleation rate of the second layer, which therefore may take place before the first layer islands have coalesced, leading to three-dimensional growth [3]. On the other hand, once three-dimensional mound-like features have formed through this (or some other) mechanism, the preferential attachment of atoms to the ascending step of the vicinal terraces on the sides of the mounds implies an effective uphill mass current, which stabilizes and amplifies the mound formation [4] (see Section IV). The ubiquity of step edge barriers on metal surfaces implies that also three-dimensional mound growth should be ubiquitous, and indeed the phenomenon has been observed, among other systems, in the homoepitaxy of Fe(100) [5,6], Rh(111) [7], Cu(100) [8,9] and Pt(111) [10].

These patterns evoke questions about the kinetic processes that determine the *shape* of individual mounds [11,12], as well as about those processes that contribute to the *coarsening* of the pattern by transferring mass from smaller mounds to larger ones [13–16]. In the present contribution we focus on the first set of questions. Starting from recent insights into the process of nucleation on top of islands [17–20], we develop a minimalistic model for the growth of a single mound, which allows us to analytically determine the asymptotic mound shape, as well as to corroborate earlier results that link the size of the topmost terrace of the mound to the rate of interlayer transport [17]. In the last section, the asymptotic mound shape is obtained as the solution of a continuum equation for the growing surface. This extends a previously established connection between macroscopic and atomistic levels of description [11] to a somewhat more realistic situation.

II. THE RATE OF SECOND LAYER NUCLEATION

A. STRONG BARRIERS, IRREVERSIBLE AGGREGATION

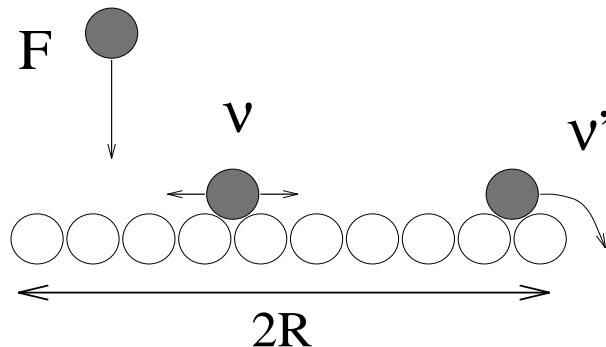


FIG. 1. Kinetic processes involved in second layer nucleation. The figure shows a circular island viewed from the side.

We consider the geometry illustrated in Figure 2. Atoms are being deposited at rate F onto a circular island of radius R . They diffuse on the island with an in-layer hopping rate ν , and descend from it with an (average) interlayer hopping rate $\nu' < \nu$. We are looking for the probability per unit time, ω , for a nucleation event to occur on the island. Assuming that dimers of adsorbed atoms are stable (as they will be at sufficiently low temperatures), nucleation takes place as soon as two adatoms meet.

The kinetic rates F , ν and ν' combine to form three relevant time scales¹: The *interarrival time*

$$\Delta t = \frac{1}{\pi R^2 F} \quad (2)$$

between subsequent depositions onto the island; the *diffusion time*

$$\tau_D \sim R^2 / \nu \quad (3)$$

required for an atom to diffuse once across the island, or for two atoms to meet; and the *residence time* τ which an atom spends on the island before descending, when no nucleation event takes place. The calculation of the residence time requires the solution of a stationary diffusion problem with appropriate boundary conditions at the step edge, which yields [3,17]

$$\tau = \frac{1}{2\nu} \left(R^2 + \frac{\nu R}{\nu'} \right). \quad (4)$$

The residence time is comparable to the diffusion time τ_D if the suppression of interlayer transport is weak, in the sense that $\nu/\nu' \ll R$, while in the opposite regime of *strong step edge barriers*, $\nu/\nu' \gg R$, the residence time becomes $\tau = R/2\nu'$ independent of ν .

We will focus on the latter regime in the following. Then $\tau \gg \tau_D$, which implies that two atoms are certain to meet once they are present simultaneously on the island. The probability for this to occur is $\tau/(\tau + \Delta t) \approx \tau/\Delta t$ if $\Delta t \gg \tau$, which is true for reasonable deposition fluxes. Multiplying this with the total number of atoms deposited onto the island per unit time, we obtain the expression [17]

$$\omega = \frac{\tau}{(\Delta t)^2} = \frac{\pi^2 F^2 R^5}{2\nu'} \quad (5)$$

for the nucleation rate, which is *exact* under the stated conditions.

B. COMPARISON WITH MEAN FIELD THEORY AND EXPERIMENTS

Equation (5) does not agree with the expression

¹Throughout lengths will be measured in units of the distance between adsorption sites on the surface.

$$\omega_{\text{mf}} = \frac{\pi}{16} \frac{\sigma F^2 \nu R^4}{\nu'^2} \quad (6)$$

derived from conventional (mean field) nucleation theory [3]; here σ denotes a dimensionless capture number of order unity. In fact ω_{mf} exceeds the true nucleation rate by a factor which is of the order of $(\nu/\nu')/R \gg 1$. The reason can be traced back to the fact that mean field nucleation theory treats the diffusing atoms as noninteracting, which implies that they continue to diffuse even after having formed a dimer, thus accumulating too many nucleation events; in general the ratio $\omega_{\text{mf}}/\omega$ is proportional to the mean number of times a site on the island is visited by an adatom during its lifetime [20].

In the analysis of experimental data, where in the past the expression (6) has mostly been used instead of (5), this overcounting implies that the value of the step edge barrier ΔE_S tends to be underestimated. For example, for Pt/Pt(111) with CO-decorated steps, the value $\Delta E_S \approx 0.36$ eV was obtained using (5), while the mean field expression (6) yields only 0.28 eV [17]. A reanalysis of a second layer nucleation study on Ag(111) [21] gave $\Delta E_S \approx 0.15$ eV instead of the estimate 0.12 eV reported in the original publication, *provided* the preexponential factor in (1) was assumed to have the conventional value $\nu'_0 = 10^{13}\text{s}^{-1}$. The attempt to determine both the step edge barrier and the prefactor by fitting the Arrhenius form (1) to data obtained at two different temperatures produces unphysically large values for ν'_0 , which indicates that the data are not sufficiently accurate for this purpose [22].

C. REVERSIBLE AGGREGATION

To some extent the above derivation of the nucleation rate can be extended to the case of reversible aggregation, where a minimum number of $i^* + 1 > 2$ atoms have to come together to form a stable nucleus [18,19]. The *encounter time* required for the atoms to meet is then no longer of the order of the diffusion time τ_D , but is (under the assumption that no metastable clusters exist) given by

$$\tau_{\text{enc}} \sim R^{2i^*} / \nu. \quad (7)$$

For $i^* > 1$ it is therefore possible that $\tau_D \ll \tau \ll \tau_{\text{enc}}$, which implies that nucleation is limited by the encounter of the atoms, rather than by their simultaneous presence on the island. The probability p_{enc} that the $i^* + 1$ atoms, once on the island, meet before one of them escapes is then of the order of $\tau/\tau_{\text{enc}} \ll 1$, while $p_{\text{enc}} \approx 1$ when $\tau \gg \tau_{\text{enc}}$. In general, the nucleation probability for a freshly deposited atom is proportional to the product of p_{enc} and the probability that i^* atoms are already present on the island. Since the latter is of the order of $(\tau/\Delta t)^{i^*}$, the nucleation rate can be written as

$$\omega \sim \frac{\tau^{i^*}}{(\Delta t)^{i^*+1}} p_{\text{enc}}. \quad (8)$$

Interestingly, in the encounter limited regime where $p_{\text{enc}} \ll 1$, this is found to coincide in order of magnitude with the prediction of mean field theory. The evaluation of (8) in the two regimes defined by the possible orderings of the relevant time scales ($\tau_D \ll \tau_{\text{enc}} \ll \tau \ll \Delta t$ or $\tau_D \ll \tau \ll \tau_{\text{enc}} \ll \Delta t$) then yields the expressions

$$\omega \approx \frac{1}{\Delta t} \left(\frac{\tau}{\Delta t} \right)^{i^*} \sim F \left(\frac{F}{\nu'} \right)^{i^*} R^{3i^*+2} \quad \text{for} \quad R \ll \left(\frac{\nu}{\nu'} \right)^\delta \quad (9)$$

$$\omega \approx \frac{1}{\tau_{\text{enc}}} \left(\frac{\tau}{\Delta t} \right)^{i^*+1} \sim F \left(\frac{F}{\nu'} \right)^{i^*} \frac{\nu}{\nu'} R^{i^*+3} \quad \text{for} \quad \left(\frac{\nu}{\nu'} \right)^\delta \ll R \ll \frac{\nu}{\nu'} \quad (10)$$

where

$$\delta = \frac{2}{2i^* - 1} < 1. \quad (11)$$

Equations (9) and (10) respectively describe the scaling regimes II and III of [18,19]. In addition, a nonstationary regime I exists, where the residence time is effectively infinite and no stationary balance between deposition and escape of atoms from the island is established, as well as a regime IV corresponding to weak step edge barriers. These regimes play no role in the context of the present paper.

III. THE WEDDING CAKE MODEL

Our model for the shape of a single mound is a stack of concentric, circular islands (Figure 3). The base is an island of radius R_0 which does not grow, and the radius of the n 'th island is denoted by R_n .

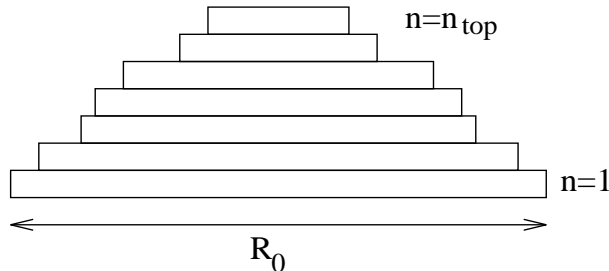


FIG. 2. A stack of concentric circular islands seen from the side.

A. RATE EQUATIONS FOR LAYER COVERAGES

The rate at which the n 'th island in the stack grows can be computed from the solution of the stationary diffusion equation for the annular region separating two islands [23]. We simplify the problem even further, and set the interlayer transport rate on the sides of the mound to zero. This is motivated by the fact (to be demonstrated below) that the mound steepens indefinitely, and hence the annular regions separating two islands become very narrow. The probability for an atom deposited in such an annular region of width l to attach to the ascending, rather than the descending step is given by [24]

$$p_+ \approx \frac{1/2 + \nu/\nu'l}{1 + \nu/\nu'l} \quad (12)$$

which tends to unity for $l \ll \nu/\nu'$. Thus interlayer transport will be increasingly suppressed as the mound steepens, and it seems reasonable to neglect it from the outset².

In the absence of interlayer transport the layer coverages $\theta_n = (R_n/R_0)^2$ satisfy the simple, *linear* equations [11,26]

$$\frac{d\theta_n}{dt} = F(\theta_{n-1} - \theta_n), \quad (13)$$

which express the fact that all atoms landing on top of the exposed part of layer $n-1$ attach to the boundary of layer n . For the top layer n_{top} descent of atoms cannot be neglected – since there are no sinks for atoms on the top layer, all atoms deposited there have to attach to the descending step. The top terrace therefore absorbs all atoms landing on layers n_{top} and $n_{\text{top}} - 1$, and grows according to

$$\frac{d\theta_{n_{\text{top}}}}{dt} = F\theta_{n_{\text{top}}-1}. \quad (14)$$

B. NUCLEATION RULES

Equations (13,14) have to be supplemented by a rule for the nucleation of a new top terrace. A simple choice would be to posit that nucleation occurs whenever the current top layer reaches some critical coverage [23]. More realistically, nucleation should be treated as a stochastic process governed by the nucleation rate ω computed in Section II. A deterministic rule which is close in spirit to stochastic nucleation can be obtained as follows. Suppose the current top terrace has nucleated at time $t = 0$, and denote its radius by $R_{\text{top}}(t)$. Then the probability that no nucleation has occurred on the top terrace up to time t is given by [17]

²In addition, setting $\nu' = 0$ makes it impossible for the boundaries of different islands in the stack to collide, which otherwise cannot generally be ruled out [25].

$$P_0(t) = \exp\left(-\int_0^t dt' \omega(R_{\text{top}}(t'))\right), \quad (15)$$

and the probability density of the time t of the next nucleation event is $-dP_0/dt$. It follows that the mean value of P_0 at the time of nucleation satisfies

$$\bar{P}_0 = \int_0^\infty dt P_0(t) \left(-\frac{dP_0}{dt}\right) = 1 - \bar{P}_0 \quad (16)$$

and thus $\bar{P}_0 = 1/2$. In the numerical implementation, we therefore monitor the increase of P_0 during the growth of the top terrace and create a new top terrace when $P_0 = 1/2$. For the nucleation rate ω the expression (5) will be used.

C. APPROXIMATE ITERATIVE SOLUTION

A full analytic solution of the model is difficult because the nucleation probability (15) depends on the size of the top terrace, which is determined by the entire history of the wedding cake through the coupled equations (13). Some first insight can be gained by assuming that the former top terrace ceases entirely to grow once a new island has nucleated on top of it. This should produce a lower bound on the island radii reached at a given time.

Denote by R_{n-1}^{top} the radius of island $n-1$ at nucleation of island n , and by t_n the time of this nucleation event. Then during its tenure as the top terrace, the radius of island n grows, according to (14), as

$$R_n(t) = \sqrt{F(t-t_n)} R_{n-1}^{\text{top}}, \quad (17)$$

and the time t_{n+1} of the next nucleation event is determined by

$$P_0(t_{n+1}) = \exp\left(-\frac{\pi^2 F^2 (R_{n-1}^{\text{top}})^5}{2\nu'} \int_{t_n}^{t_{n+1}} dt [F(t-t_n)]^{5/2}\right) = 1/2. \quad (18)$$

This implies a recursion relation

$$R_n^{\text{top}} = R_c^{5/7} (R_{n-1}^{\text{top}})^{2/7} \quad (19)$$

for the size of the top terrace at nucleation of the next layer, where we have introduced the characteristic radius

$$R_c = \left(\frac{7 \ln 2}{\pi^2}\right)^{1/5} \left(\frac{\nu'}{F}\right)^{1/5} \approx 0.868 \cdot \left(\frac{\nu'}{F}\right)^{1/5}. \quad (20)$$

The time interval $\tau_n = t_{n+1} - t_n$ during which $n_{\text{top}} = n$ is related to R_n^{top} through (17), and correspondingly satisfies

$$\tau_{n+1} = F^{-1} (F \tau_n)^{4/7}. \quad (21)$$

It is easy to check that the recursion relations (19) and (21) approach fixed point values

$$R_n^{\text{top}} \rightarrow R_c, \quad F \tau_n \rightarrow 1 \quad (22)$$

exponentially fast in n . Thus asymptotically there is one nucleation event during the growth of one monolayer³, and nucleation occurs when the radius of the top terrace has reached the value R_c . We shall see below that these statements remain valid for the full dynamics, although the approach of R_n^{top} and τ_n to their asymptotic values is slower than exponential due to the coupling to the lower layers.

³This has also been observed experimentally for engineered mounds grown on Cu(100) [27].

D. NUMERICAL INTEGRATION

Since the deposition flux F and the size R_0 of the base of the mound can be eliminated by rescaling the time and the island radii, the model effectively contains only the single parameter ν'/F . For convenience we will express this parameter through the coverage θ_c of the top layer at nucleation, which is given by

$$\theta_c = \left(\frac{R_c}{R_0}\right)^2 = \left(\frac{7 \ln 2}{\pi^2}\right)^{2/5} \frac{(\nu')^{2/5}}{F^{2/5} R_0^2}. \quad (23)$$

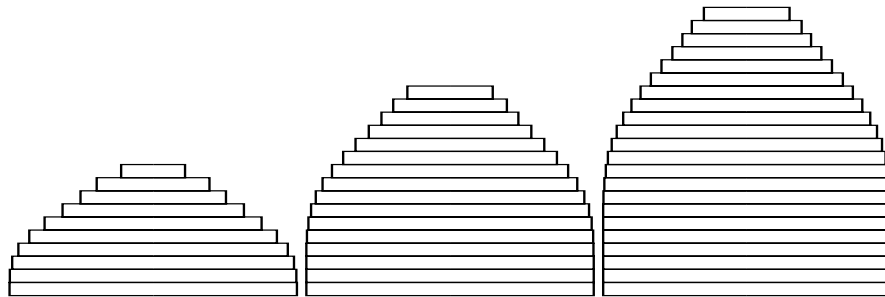


FIG. 3. Wedding cakes grown numerically with $\theta_c = 0.1$, at total coverages of $Ft = 5, 10$ and 15 monolayers. The figure shows a stack of circular islands seen from the side, i.e. the bar at level n has a length proportional to $\sqrt{\theta_n}$.

Figure 4 shows the result of a numerical integration of the model equations for $\theta_c = 0.1$. The figure suggests that the number of exposed layers (with coverages $0 < \theta_n < 1$) increases with time. This is quantified in Fig.5, which shows the evolution of the surface width

$$W^2(t) = \sum_{n=1}^{\infty} (n - Ft)^2 (\theta_{n-1} - \theta_n). \quad (24)$$

In the case of purely statistical growth with $\nu' = \theta_c = 0$, $W^2 = Ft$ because the exposed coverages $\theta_{n-1} - \theta_n$ are given by a Poisson distribution with parameter Ft [11,26]. Figure 5 shows that also for $\theta_c > 0$ the squared width grows linearly in Ft , but with a coefficient that is less than unity; in Section III E it will be shown that the coefficient is simply $1 - \theta_c$. Since the lateral mound size is fixed, the unbounded increase of $W(t)$ implies that the mounds steepen indefinitely, with the terrace width on the mound slopes decreasing as $1/\sqrt{Ft}$; a quantitative expression is given in (32).

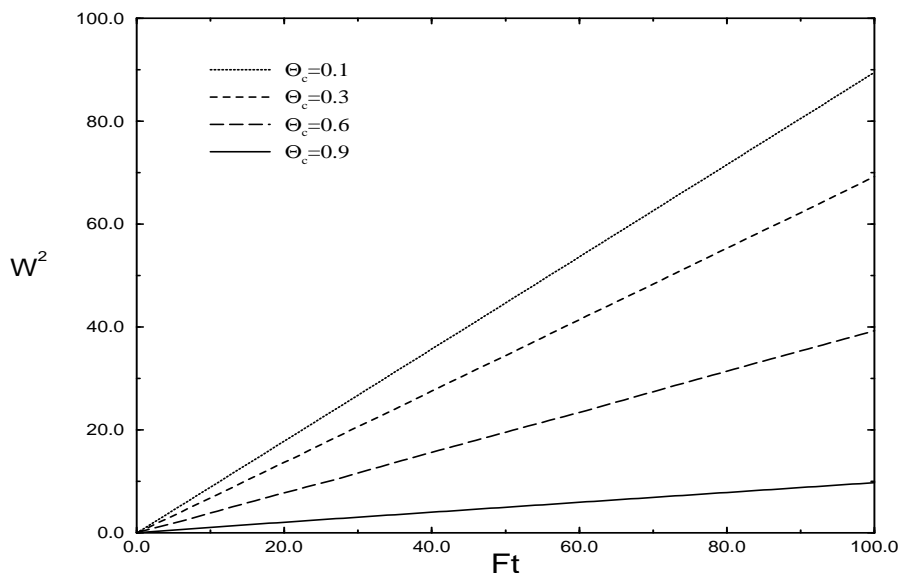


FIG. 4. Surface width (24) as a function of time.

Finally, Fig.6 illustrates the convergence of the top terrace size at nucleation, and the time intervals between subsequent nucleation events, to their limiting values predicted by (22). As might be expected from the behavior of the surface width, the convergence is linear in $1/\sqrt{Ft}$, rather than exponential.

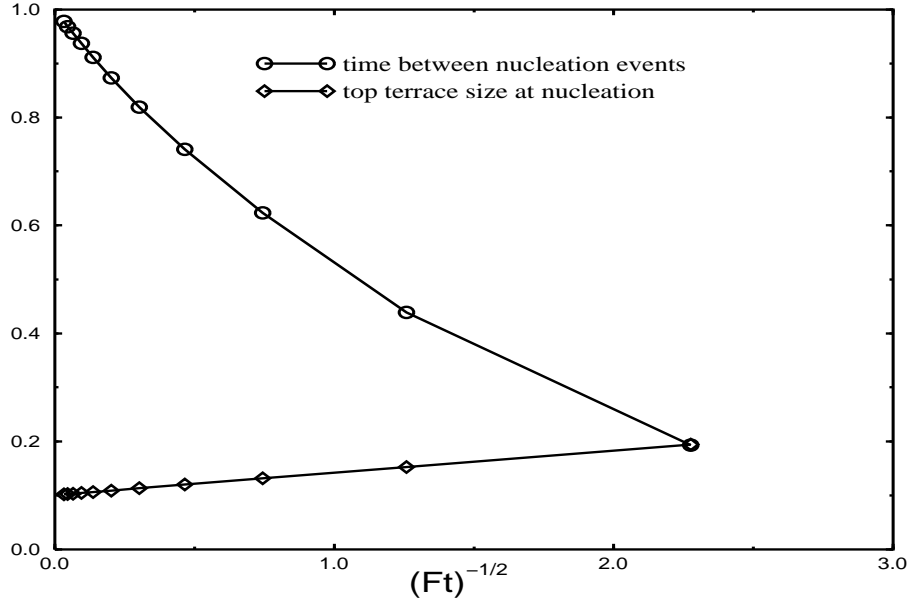


FIG. 5. Convergence of the time between nucleation events, and the top terrace size at nucleation, as a function of $1/\sqrt{Ft}$.

E. THE ASYMPTOTIC MOUND SHAPE

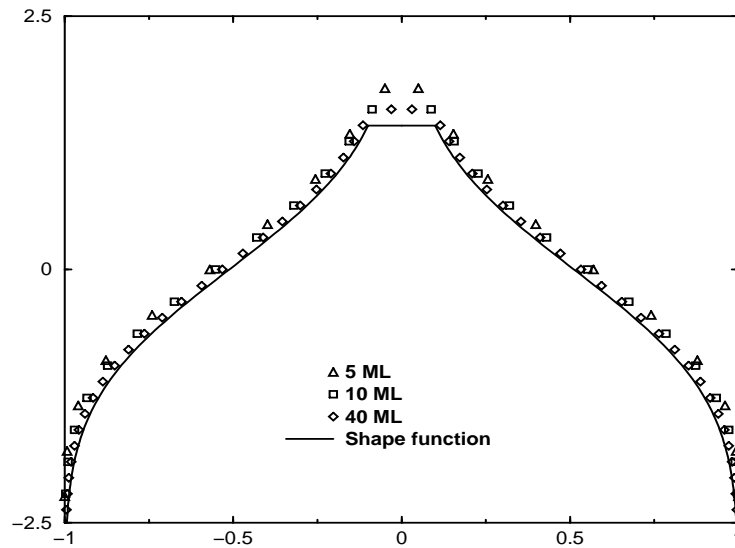


FIG. 6. Convergence of numerically generated wedding cakes to the asymptotic shape function $\Phi(x)$. The symbols show the coverage profile rescaled according to (25).

The numerical solution of the model equations shows that the height profile of the mound converges to a time-independent asymptotic shape, when viewed relative to the mean film height Ft and rescaled horizontally by \sqrt{Ft} to compensate the increase of the surface width (Figure 7). To derive the shape analytically, we write the coverage profile $\theta_n(t)$ as a traveling wave of width \sqrt{Ft} ,

$$\theta_n(t) = \Phi[(n - t)/\sqrt{Ft}]. \quad (25)$$

Inserting this into (13) and expanding for large Ft one finds that the shape function $\Phi(x)$ has to satisfy the differential equation

$$\Phi''(x) = -x\Phi'(x), \quad (26)$$

where $x = (n - t)/\sqrt{Ft}$ is the scaling variable. This shows that the inflection point of the profile, where $\Phi'' = 0$, is always located at $x = 0$, i.e. at $n = Ft$. The solution of (26) which satisfies the boundary condition $\lim_{x \rightarrow -\infty} \Phi(x) = 1$ reads

$$\Phi(x) = 1 - \sqrt{\frac{2}{\pi}} C \int_{-\infty}^x dy e^{-y^2/2} = 1 - C[1 + \operatorname{erf}(x/\sqrt{2})], \quad (27)$$

where $\operatorname{erf}(s)$ denotes the error function, and C is a constant of integration. The profile is cut off at the rescaled height x_{\max} of the top terrace, where the coverage takes the value θ_c ,

$$\Phi(x_{\max}) = \theta_c. \quad (28)$$

Accordingly, the height of the top terrace above the mean film thickness Ft is $x_{\max}\sqrt{Ft}$.

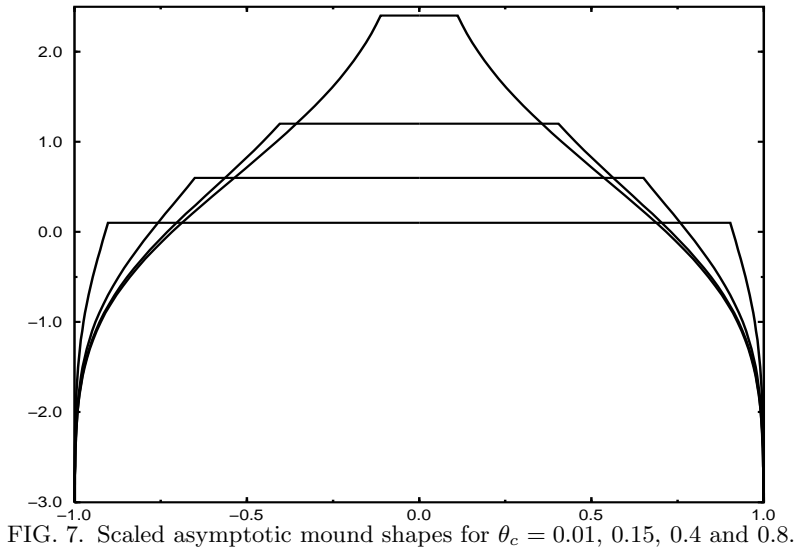


FIG. 7. Scaled asymptotic mound shapes for $\theta_c = 0.01, 0.15, 0.4$ and 0.8 .

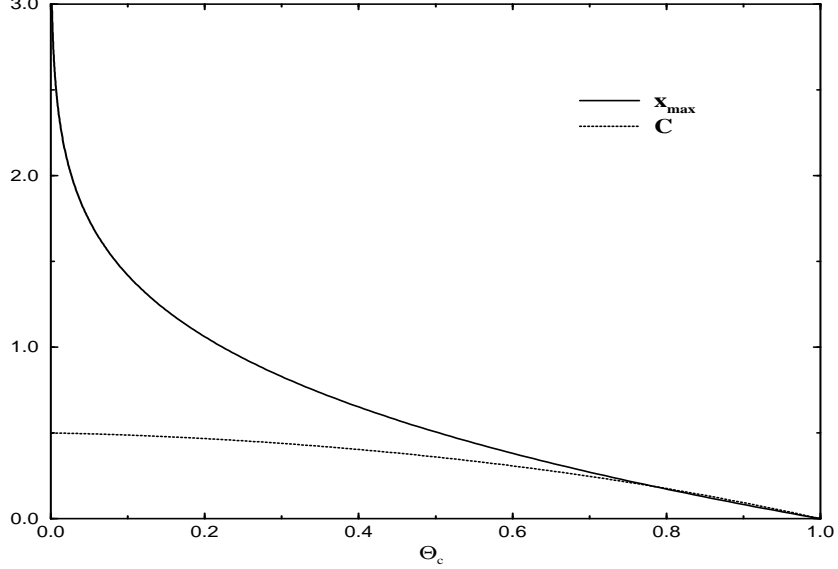


FIG. 8. Shape parameters C and x_{\max} as a function of θ_c .

The two parameters C and x_{\max} of the shape function are related by (28), but to fix both of them a further relation is required. This is provided by the normalization condition

$$\sum_{n=1}^{\infty} \theta_n = Ft, \quad (29)$$

which, using (25), translates into

$$\int_0^{x_{\max}} dx \Phi(x) = \int_{-\infty}^0 dx (1 - \Phi(x)). \quad (30)$$

Together equations (27,28,30) define a family of shape functions parametrized by θ_c . Examples of these functions are shown in Fig.8, while Fig.9 illustrates the dependence of x_{\max} and C on θ_c . For the case of Pt growth on Pt(111) at 440 K, the experimentally determined mean mound shape has been compared to the scaling function $\Phi(x)$ for $\theta_c = 0$, and good agreement was found except near the top of the mound [10]. Evaluation of the top terrace size and comparison with (20) yields the estimate $\Delta E_S \approx 0.25$ eV [28].

Other features of the mound shape can be easily extracted. The surface width (24) turns out to be given by

$$W^2 \approx (1 - \theta_c)Ft \quad (31)$$

asymptotically. The mound radius at the level of the mean film thickness, $x = 0$, is given by $\sqrt{1 - C}R_0$, and the maximum terrace width on the mound slopes, located also at the inflection point $x = 0$, decreases with increasing film thickness according to

$$l_{\max}/R_0 \approx \frac{\Phi'(0)}{2\sqrt{\Phi(0)}} \frac{1}{\sqrt{Ft}} = \frac{C}{\sqrt{2\pi(1-C)}} \frac{1}{\sqrt{Ft}}. \quad (32)$$

F. THE DISTRIBUTION OF TOP TERRACE SIZES

In an image of a multilayer film subject to the mound instability one will typically see top terraces of a range of sizes, because they are caught in different stages of their evolution. In [17] a simple model for the size distribution was developed, which decouples the dynamics of the top terrace from the rest of the mound by assuming that each top terrace grows on a template – the base terrace – of constant radius R_b . The nucleation probability (15) is then evaluated with

$$R_{\text{top}}(t) = \sqrt{Ft} R_b, \quad (33)$$

and its derivative $-dP_0/dt$ is interpreted as the probability distribution for the time intervals between two subsequent nucleation events. The base terrace radius is fixed through the requirement that the mean time between nucleation events equals the monolayer deposition time, which implies

$$F \int_0^\infty dt P_0(t) = 1. \quad (34)$$

One obtains $R_b \approx 0.867 \cdot (\nu'/F)^{1/5}$, which is virtually indistinguishable from the expression (20) derived from the condition $P_0 = 1/2$. If one demands instead that nucleation takes place at the maximum of the probability density, i.e. at the time determined by $d^2P_0/dt^2 = 0$, a prefactor of 0.873 is obtained. All reasonable criteria give the same result, because the probability density $-dP_0/dt$ is sharply peaked around its maximum.

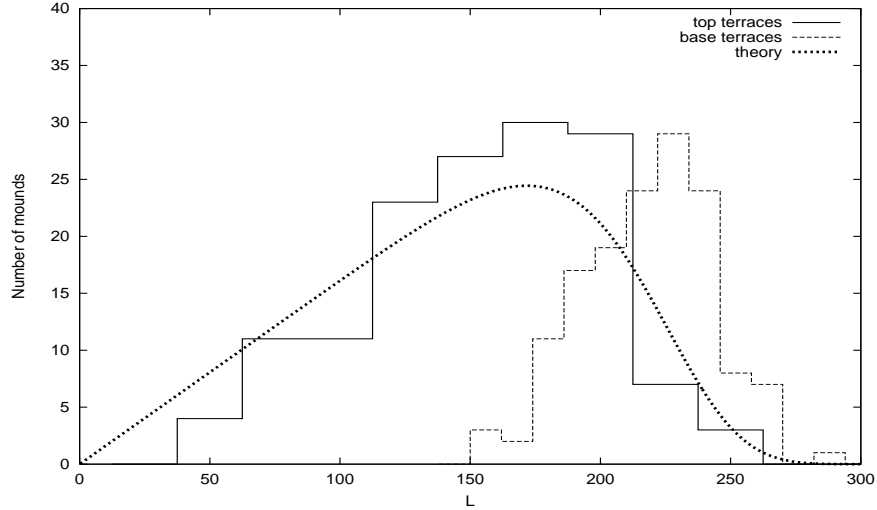


FIG. 9. Distribution of sizes of top terraces, measured in terms of their perimeter L in units of lattice sites [17]. The full line shows a histogram obtained from the evaluation of STM images of 145 mounds, grown at 440 K in the presence of a partial CO pressure of 1.9×10^{-9} mbar, at a total coverage of 37.1 monolayers. The thick dotted line shows the (appropriately normalized) prediction (35). The thin dashed line shows the corresponding histogram for the base terraces, i.e. the terraces supporting the top terraces. It has been included to demonstrate that the assumption of a constant size of base terraces is reasonable.

Within this model, the probability $P(R)$ to observe a top terrace of size R is equal to the probability that the time since the last nucleation event is *at least* $F^{-1}(R/R_b)^2$, which equals $P_0(F^{-1}(R/R_b)^2)$. Changing variables from t to R then yields

$$P(R) = \frac{2R}{FR_b^2} \exp\left(-\frac{\pi^2 FR^7}{7\nu'R_b^2}\right). \quad (35)$$

As can be seen in Fig.10, this gives a quite satisfactory description of the experimental data. By fitting the mean of (35), the step edge barrier for Pt(111) in the presence of CO has been extracted from images of multilayer mounds [17]. The result $\Delta E_S \approx 0.33$ eV is in good agreement with the estimate of 0.36 eV obtained from second layer nucleation in the submonolayer regime (see Section II).

G. THE TOP TERRACE SIZE FOR REVERSIBLE AGGREGATION

The derivation of (20) can be repeated using the expressions (9,10) for the nucleation rate in the case of reversible aggregation, $i^* > 1$ [19]. In general the top terrace size is given by an expression of the form

$$R_c \sim \left(\frac{\nu}{F}\right)^{\gamma'} \left(\frac{\nu'}{\nu}\right)^{\mu'}, \quad (36)$$

where the exponents γ' and μ' take the values

$$\gamma' = \mu' = \frac{i^*}{3i^* + 2} \quad (\text{regime II}) \quad (37)$$

$$\gamma' = \frac{i^*}{i^* + 3}, \quad \mu' = \frac{i^* + 1}{i^* + 3} \quad (\text{regime III}) \quad (38)$$

In terms of the kinetic rates ν , ν' and F , the two regimes are defined by the inequalities $F/\nu \ll \nu'/\nu \ll (F/\nu)^{\delta_1}$ (regime II) and $(F/\nu)^{\delta_1} \ll \nu'/\nu \ll (F/\nu)^{\chi/2}$ (regime III), where

$$\delta_1 = \frac{i^*(2i^* - 1)}{2i^*(i^* + 1) + 2} \quad (39)$$

and

$$\chi = \frac{i^*}{i^* + 2} \quad (40)$$

is the island density exponent of classical nucleation theory, which relates the density N of first layer islands to the ratio F/ν through [29]

$$N \sim \left(\frac{\nu}{F}\right)^\chi. \quad (41)$$

IV. CONTINUUM THEORY

The continuum theory of mound formation is based on the notion of a growth-induced, uphill surface current [4,24,30,31]. Figure 11 illustrates the basic idea: Because atoms deposited onto a vicinal terrace on the side of a mound attach preferentially to the ascending step, they travel on average in the direction of the uphill slope⁴ between the point of deposition and the point of incorporation.

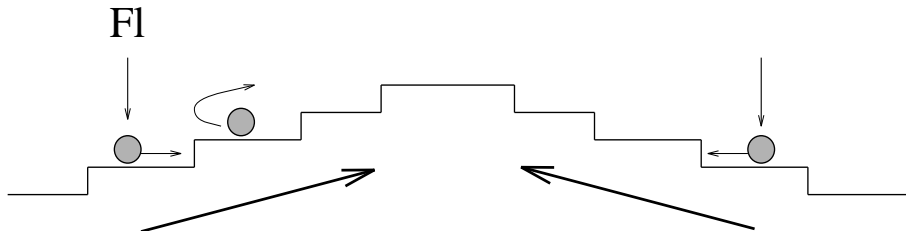


FIG. 10. Illustration of the uphill surface current generated by step edge barriers.

The evaluation of the current is particularly simple when interlayer transport is completely suppressed, and nucleation on the vicinal terrace can be neglected⁵. An atom deposited onto a vicinal terrace of width l then travels an average distance $l/2$ to the ascending step, and hence the current is $Fl/2$. Describing the surface profile by a continuous height function $h(\vec{r}, t)$ which measures the film thickness (in units of the monolayer thickness) above a substrate point \vec{r} , the local terrace width is $l = |\nabla h|^{-1}$, and hence the current is given by the expression

$$\vec{J} = \frac{F}{2|\nabla h|^2} \nabla h. \quad (42)$$

The surface profile evolves according to the continuity equation

⁴It is important to realize that this does *not* require atoms to actually climb uphill across steps [30].

⁵Expressions for more general situations are derived in [24,31].

$$\frac{\partial h}{\partial t} + \nabla \cdot \vec{J} = F. \quad (43)$$

Here we are specifically interested in radially symmetric mounds. Rewriting (43) in polar coordinates and using (42) yields the following evolution equation for the mound profile $h(r, t)$:

$$\frac{\partial h}{\partial t} = -\frac{F}{2r} \frac{\partial}{\partial r} r \left(\frac{\partial h}{\partial r} \right)^{-1} + F. \quad (44)$$

We want to show that (44) possesses solutions corresponding to the asymptotic mound shape derived in Section III E. To this end we make the ansatz

$$h(r, t) = \sqrt{Ft} \psi(r) + Ft. \quad (45)$$

Inserting this into (44) yields the differential equation

$$\frac{d}{dr} \left(\frac{r}{\psi'(r)} \right) = r\psi(r). \quad (46)$$

In order to establish the equivalence between the shapes described by $\psi(r)$ and the scaled coverage distribution $\Phi(x)$ of Section III E, we need to verify that the function $\psi(r)$ defined implicitly by

$$\left(\frac{r}{R_0} \right)^2 = \Phi(\psi(r)) \quad (47)$$

solves (46). Indeed, taking the derivative with respect to ψ on both sides yields

$$r \left(\frac{d\psi}{dr} \right)^{-1} = -\frac{CR_0^2}{2} e^{-\psi^2/2} \quad (48)$$

which reduces to (46) upon taking another derivative with respect to r .

This calculation shows explicitly that the sides of the mounds evolve according to the continuum equation (43); in [11] the same result was obtained for a one-dimensional geometry. The continuum description does however not include the nucleation on the top terraces, which have to be added to the profile determined by (46) as a boundary condition. The development of a continuum theory of epitaxial growth which explicitly incorporates nucleation remains a challenge for the future.

Acknowledgements. Part of this paper is based on joint work with Thomas Michely and Paolo Politi. Support by DFG within SFB 237 *Unordnung und grosse Fluktuationen* is gratefully acknowledged.

- [1] G. Ehrlich and F. Hudda, *J. Chem. Phys.* **44** (1966) 1039
- [2] R.L. Schwoebel and E.J. Shipsey, *J. Appl. Phys.* **37** (1966) 3682
- [3] J. Tersoff, A.W. Denier van der Gon and R.M. Tromp, *Phys. Rev. Lett.* **72** (1994) 266
- [4] J. Villain, *J. Phys. I France* **1** (1991) 19
- [5] K. Thürmer, R. Koch, M. Weber and K.H. Rieder, *Phys. Rev. Lett.* **75** (1995) 1767
- [6] J. A. Strosio, D. T. Pierce, M.D. Stiles, A. Zangwill and L.M. Sander, *Phys. Rev. Lett.* **75** (1995) 4246
- [7] F. Tsui, J. Wellman, C. Uher and R. Clarke, *Phys. Rev. Lett.* **76** (1996) 3164
- [8] H.-J. Ernst, F. Fabre, R. Folkerts and J. Lapujoulade, *Phys. Rev. Lett.* **72** (1994) 112
- [9] J.-K. Zuo and J.F. Wendelken, *Phys. Rev. Lett.* **78** (1997) 2791
- [10] M. Kalf, P. Šmilauer, G. Comsa and T. Michely, *Surf. Sci.* **426** (1999) L447
- [11] J. Krug, *J. Stat. Phys.* **87** (1997) 505
- [12] P. Politi, *J. Phys. I* **17** (1997) 797
- [13] L.-H. Tang, P. Šmilauer and D.D. Vvedensky, *Eur. Phys. J. B* **2** (1998) 409
- [14] M. Siegert, *Phys. Rev. Lett.* **81** (1998) 5481
- [15] D. Moldovan and L. Golubovic, *Phys. Rev. E* **61** (2000) 6190

- [16] Th. Michely, M. Kalff, G. Comsa, M. Strobel and K.-H. Heinig, *Phys. Rev. Lett.* **86** (2001) 2589
- [17] J. Krug, P. Politi and T. Michely, *Phys. Rev. B* **61** (2000) 14037
- [18] S. Heinrichs, J. Rottler and P. Maass, *Phys. Rev. B* **62** (2000) 8338
- [19] J. Krug, *Eur. Phys. J. B* **18** (2000) 713
- [20] C. Castellano and P. Politi, *cond-mat/0102212* (2001)
- [21] K. Bromann, H. Brune, H. Röder and K. Kern, *Phys. Rev. Lett.* **75** (1995) 677
- [22] J. Krug, *cond-mat/0008451* (2000)
- [23] J.A. Meyer, J. Vrijmoeth, H.A. van der Vlegt, E. Vlieg and R.J. Behm, *Phys. Rev. B* **51** (1995) 14790
- [24] J. Krug, *Adv. Phys.* **46** (1997) 139
- [25] H.-J. Gossmann, F.W. Sinden and L.C. Feldman, *J. Appl. Phys.* **67** (1990) 745
- [26] P.I. Cohen, G.S. Petrich, P.R. Pukite, G.J. Whaley and A.S. Arrott, *Surf. Sci.* **216** (1989) 222
- [27] R. Gerlach, T. Maroutian, L. Douillard, D. Martinotti and H.-J. Ernst, *Surf. Sci.* (in the press)
- [28] T. Michely, M. Kalff, J. Krug and P. Politi, *Physikalische Blätter* **55** (1999) Nr.11, p. 53
- [29] J. A. Venables, G. D. T. Spiller and M. Hanbücken, *Rep. Prog. Phys.* **47** (1984) 399
- [30] J. Krug, M. Plischke and M. Siegert, *Phys. Rev. Lett.* **70** (1993) 3271
- [31] P. Politi, G. Grenet, A. Marty, A. Ponchet and J. Villain, *Phys. Rep.* **324** (2000) 271